Generation of continuous complex-valued functions for a joint transform correlator

Rafael Piestun, Joseph Rosen, and Joseph Shamir

The principle of representing continuous complex-valued functions by their decomposition into three positive-valued ones is proposed for the generation of complex reference functions for a joint transform correlator. Three basic approaches involving coherent and incoherent superposition of the component functions are analyzed. The potentials and limitations of the techniques are discussed.

1. Introduction

One can usually implement a joint transform correlator (JTC)[1] by using positive inputs and references. Earlier work has indicated that the projection of complex-valued reference functions onto the input plane can enhance the performance of these correlators.[2–4] Unfortunately, with current technology only holographic methods are available for implementing complex-valued functions. These are inconvenient because of the large space–bandwidth product required and the need to work off axis with limited diffraction efficiency.

The decomposition of a complex function into positive-valued functions has been proposed in the past for incoherent processing[5] and used in the encoding of computer-generated holograms.[6] In this paper we propose to generate continuous complex reference functions for the JTC that employs a three-component decomposition.

Three planes are distinguished in the JTC, namely, the input plane where the target and reference function are placed, the Fourier plane where the joint transform hologram (JTH) is recorded, and the output or correlation plane. On each of these planes it is possible to superpose the partial results obtained with each component function at the input.

Accordingly, three basic techniques are presented and compared in what follows. The first involves coherent superposition of the component real functions at the input plane to obtain a single joint spectrum. The second is the incoherent addition of joint spectra obtained with the component functions, whereas in the third method the correlations with the three-component functions are superposed.

The theoretical basis and methodology are described in Section 2, whereas computer simulations and preliminary experiments are presented in Section 3. Discussion and conclusions are given in Section 4.

2. Theory and Procedures

The basic idea behind our procedure is to generate a complex wave front by the superposition of phase-shifted real functions. It is well known that any complex function $h(x, y) = |h(x, y)|\exp[\phi(x, y)]$ can be decomposed, in the complex plane, into two real functions, $h_1(x, y)$ and $h_2(x, y)$, along two orthogonal directions. However, since we assume that only positive values can be produced with transparencies, this procedure must be modified.

One possibility to implement a full complex-valued reference function, using only two positive functions with a constant phase difference between them, is to reduce the dynamic range of the component functions by adding a bias [Fig. 1(a)]. Unfortunately, such a bias is also transferred to the correlation plane of a JTC leading to a substantial degradation of the signal-to-noise ratio. A better alternative is to consider the decomposition into three positive functions

J. Rosen is with the Optical Signal Processing Branch, Rome Laboratory, Hanscom Air Force Base, Massachusetts 01731-5000; the other authors are with the Department of Electrical Engineering, Technion–Israel Institute of Technology, Haifa 32000, Israel.
Received 17 February 1993; revised manuscript received 29 November 1993.
0003-6935/94/204398-08$06.00/0.

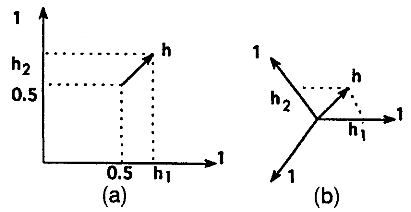

Fig. 1. Representation of a complex function by real positive functions: (a) addition of a bias to the real and imaginary components with reduction of the available dynamic range, (b) decomposition into three functions along constant phasors.

[Fig. 1(b)], to be superposed later with constant phase differences:

$$h(x, y) = h_1(x, y) + h_2(x, y)\exp\left(i\,\frac{2\pi}{3}\right) + h_3(x, y)\exp\left(i\,\frac{4\pi}{3}\right). \quad (1)$$

The function $h(x, y)$ can be generated by the three real and positive components using coherent superposition in an interferometerlike setup. We show in Subsections 2.B and 2.C that in a JTC the procedure can also be implemented by incoherent superposition.

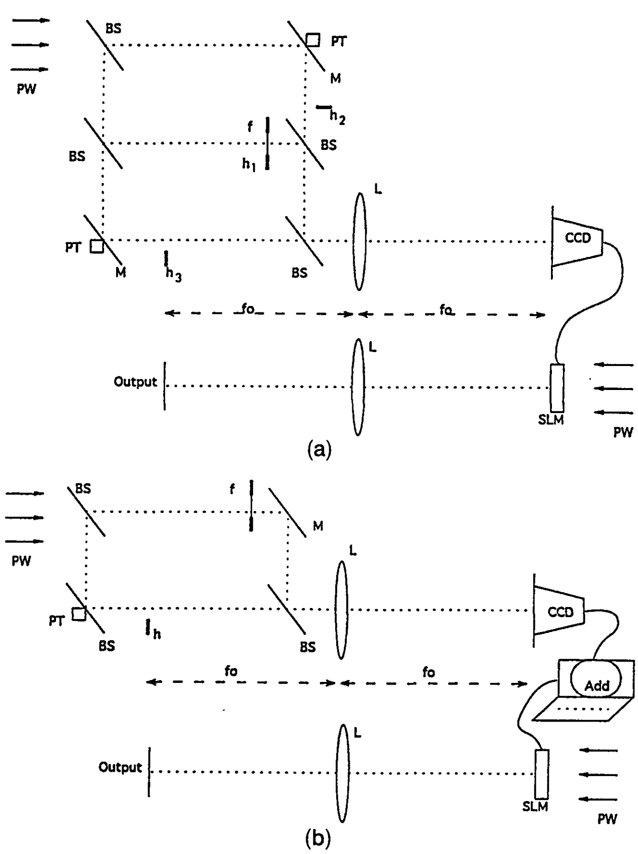

Fig. 2. Interferometric arrangements to perform correlation with complex references through (a) coherent superposition, (b) incoherent superposition. PT, piezoelectric transducer; M, mirror; BS, beam splitter; L, lens; f, focal length of L; PW, plane wave. h_1, h_2, h_3, and f are positive transparencies.

A. Superposition at the Input Plane

The complex function can be generated through coherent superposition of the wave fronts that come from the component functions in an interferometric arrangement, as indicated in Fig. 2(a), which shows an interferometer composed of three arms, each containing a different transparency, h_1, h_2, and h_3. The transparencies are aligned and at equal optical distances d from the output beam splitter. The field in the Fourier plane can be written taking into account the linear property of the Fourier transform (FT):

$$\mathscr{F}\{h_1(x, y) + f(x, y + b)\} + \mathscr{F}\{h_2(x, y)\exp(i\phi_2)\} + \mathscr{F}\{h_3(x, y)\exp(i\phi_3)\} = H(u, v) + F(u, v)\exp(i2\pi bv), \quad (2)$$

where $\phi_2 = 2\pi/3$ and $\phi_3 = 4\pi/3$ are the phase differences among the arms of the interferometer, and b is the in-plane separation of f and h. Recording this field in a square-law detector yields the joint spectrum of f and h.

Note that not only the reference can be made complex, but also the object function f.

B. Superposition at the Fourier Plane

The interesting region of the output plane in a classical JTC is the cross correlation, $f \star h$, of the input (f) and the reference (h). Suppose we place h_1 in the input plane, together with f, register the Fourier plane intensity pattern, and proceed in the same way with h_2 and f. If we sum both spectra (incoherent superposition) and perform the FT of the result, we obtain the correlation $f \star (h_1 + h_2)$ at the output plane. This follows from the linearity of the FT, as is also discussed below.

To apply the above property to an arbitrary complex function h, we decompose it as in Eq. (1). Each component can be presented separately, with its corresponding phase, at the input of a JTC together with the input function $f(x, y)$. For example, if we place $h_2(x, y)\exp(i2\pi/3)$ at a distance b from $f(x, y)$, we obtain, in the Fourier plane, the intensity distribution

$$|F + H_2|^2 = |F|^2 + |H_2|^2 + |F||H_2| \times \exp\left\{i\left[2\pi bv + \phi_F(u, v) - \phi_2(u, v) - \frac{2\pi}{3}\right]\right\} + |F||H_2|\exp\left\{-i\left[2\pi bv + \phi_F(u, v) - \phi_2(u, v) - \frac{2\pi}{3}\right]\right\}, \quad (3)$$

where $|F|\exp(i\phi_F)$ and $|H_2|\exp(i\phi_2)$ are the FT's of $f(x, y)$ and $h_2(x, y)$, respectively. Proceeding in the same way with h_1 and h_3 and adding the three results we obtain

$$\begin{aligned}\Sigma_i |F + H_i|^2 = {} & 3|F|^2 + |H_1|^2 + |H_2|^2 + |H_3|^2 \\ & + |F||H_1|\exp[i(2\pi bv + \phi_F - \phi_1)] \\ & + |F||H_1|\exp[-i(2\pi bv + \phi_F - \phi_1)] \\ & + |F||H_2|\exp\left[i\left(2\pi bv + \phi_F - \phi_2 - \frac{2\pi}{3}\right)\right] \\ & + |F||H_2|\exp\left[-i\left(2\pi bv + \phi_F - \phi_2 - \frac{2\pi}{3}\right)\right] \\ & + |F||H_3|\exp\left[i\left(2\pi bv + \phi_F - \phi_3 - \frac{4\pi}{3}\right)\right] \\ & + |F||H_3|\exp\left[-i\left(2\pi bv + \phi_F - \phi_3 - \frac{4\pi}{3}\right)\right] . \end{aligned} \quad (4)$$

We obtained the complex amplitude distribution over the output plane of the JTC by performing a FT of the expression in Eq. (4):

$$\begin{aligned} c(x, y) = {} & 3f \star f + h_1 \star h_1 + h_2 \star h_2 + h_3 \star h_3 \\ & + f(x, y) \star \left[h_1(x, y) + h_2(x, y)\exp\left(i\frac{2\pi}{3}\right) + h_3(x, y)\exp\left(i\frac{4\pi}{3}\right)\right] * \delta(x, y - b) \\ & + f(-x, -y) \star \left[h_1(-x, -y) + h_2(-x, -y)\exp\left(-i\frac{2\pi}{3}\right) + h_3(-x, -y)\exp\left(-i\frac{4\pi}{3}\right)\right] * \delta(x, y + b), \end{aligned} \quad (5)$$

where we have used the hermitic property of the FT and the fact that the FT of F^*H equals $[f \star h](x, y)$. $\star$ and $*$ are the symbols for correlation and convolution, respectively. Substituting Eq. (1) into Eq. (5) yields the last and desired result:

$$\begin{aligned} c(x, y) = {} & 3f \star f + h_1 \star h_1 + h_2 \star h_2 + h_3 \star h_3 \\ & + f(x, y) \star h(x, y) * \delta(x, y - b) + f(-x, -y) \\ & \star h^*(-x, -y) * \delta(x, y + b). \end{aligned} \quad (6)$$

It is important to note that the last two terms of Eq. (6), which correspond to the correlations $f \star h$ and $h \star f$, are separated from each other and from the other terms in the output plane. It is therefore possible to treat them independently.

C. Superposition at the Correlation Plane

Superposition at the output plane of the JTC can be done by taking advantage of the linearity of the correlation operation. The complex filter h is decomposed again as in Eq. (1) and three correlations in a regular JTC arrangement are performed, leading to

$$c_k = f \star h_k, \qquad k = 1, 2, 3. \quad (7)$$

Coherent superposition is possible by adding Fourier lenses to the interferometric arrangement described in Subsection 2.A. Correlation c is obtained according to the equation

$$c = f \star h = c_1(x, y) + c_2(x, y)\exp\left(i\frac{2\pi}{3}\right) + c_3(x, y)\exp\left(i\frac{4\pi}{3}\right) . \quad (8)$$

The implementation of this procedure, however, is difficult, and a much simpler procedure consists of separate detection of the three correlations c_k^2 and their numerical superposition in a digital computer to obtain either c or $|c|^2$. Since both f and h_k are positive and real, the c_k are also positive real and the c_k^2 contain all the necessary information. c can be calculated as in Eq. (8) and the squared amplitude can be calculated as follows:

$$|c|^2 = c_1^2 + c_2^2 + c_3^2 - c_1c_2 - c_1c_3 - c_2c_3. \quad (9)$$

Superposition at the correlation plane with two composing functions for the specific case of a circular harmonic expansion filter has been proposed by Yu *et al.*[7]

D. Optical Implementation

All component functions h_i are real and positive and thus may be displayed on spatial light modulators (SLM's) or as transparencies.

For coherent superposition at the input plane, it is possible to use the configuration of Fig. 2(a) to achieve separate optical paths for the transparencies. The path differences can be adjusted by placing the mirrors on piezoelectric transducers or by inserting transparent plates or electro-optic materials to produce the constant phase shifts required. Consequently the system will behave as if the input reference were the complex function $h(x, y)$.

The same architecture is also convenient for incoherent superposition at the Fourier plane for which only two arms are needed. Figure 2(b) depicts a possible setup. Alternative placement of the h_i's on the same channel, while the object function is on the other channel, yields three different JTH's [see Eq. (4)] that can be digitally recorded and added in a computer. Before each recording, a $\lambda/3$ shift is performed with the piezoelectric mirror. Displaying the result on a SLM in a FT system gives the correlation of target f and reference h (now a complex function) and other terms as seen from Eq. (6). A regular JTC configuration can also be used when the phase lags are obtained with phase plates.

Alternatively, a simple approximate implementation can be obtained under the assumption that the distance b between the input and the filter is big enough compared to their dimensions along the separation axis. Three regular JTH's produced with f and h_k ($k = 1, 2, 3$) are digitally recorded. The JTH corresponding to f and h_2 is translated a distance $1/3b$ in the spatial frequency domain, leading to

$$\begin{aligned}\mathrm{JTH2} &= |F + H_2|^2\left(u, v - \frac{1}{3b}\right) \\ &= \left|F\left(u, v - \frac{1}{3b}\right)\right|^2 + \left|H_2\left(u, v - \frac{1}{3b}\right)\right|^2 \\ &\quad + \left|F\left(u, v - \frac{1}{3b}\right)\right|\left|H_2\left(u, v - \frac{1}{3b}\right)\right| \\ &\quad \times \exp\left\{i\left[2\pi b\left(v - \frac{1}{3b}\right)\right.\right. \\ &\quad \left.\left. + \phi_F\left(u, v - \frac{1}{3b}\right) - \phi_2\left(u, v - \frac{1}{3b}\right)\right]\right\} \\ &\quad + \left|F\left(u, v - \frac{1}{3b}\right)\right|\left|H_2\left(u, v - \frac{1}{3b}\right)\right| \\ &\quad \times \exp\left\{-i\left[2\pi b\left(v - \frac{1}{3b}\right)\right.\right. \\ &\quad \left.\left. + \phi_F\left(u, v - \frac{1}{3b}\right) - \phi_2\left(u, v - \frac{1}{3b}\right)\right]\right\}. \end{aligned} \tag{10}$$

The JTH of f and h_3 is translated in the same way to $2/(3b)$ and the three spectra are added. To see the final result we calculate the FT of one of the translated JTH's:

$$\begin{aligned}&\mathscr{F}\{\mathrm{JTH2}\} \\ &= f(x, y)\exp\left[-i\left(\frac{2\pi}{3b}\right)y\right] \star f(x, y)\exp\left[-i\left(\frac{2\pi}{3b}\right)y\right] \\ &\quad + h(x, y)\exp\left[-i\left(\frac{2\pi}{3b}\right)y\right] \star h(x, y)\exp\left[-i\left(\frac{2\pi}{3b}\right)y\right] \\ &\quad + f(-x, -y)\exp\left[i\left(\frac{2\pi}{3b}\right)y\right] \star h(-x, -y) \\ &\quad \times \exp\left[i\left(\frac{2\pi}{3b}\right)y\right] \star \delta(x, y + b)\exp\left(-i\,\frac{2\pi}{3}\right) \\ &\quad + f(x, y)\exp\left[-i\left(\frac{2\pi}{3b}\right)y\right] \star h(x, y) \\ &\quad \times \exp\left[-i\left(\frac{2\pi}{3b}\right)y\right] \star \delta(x, y - b)\exp\left(i\,\frac{2\pi}{3}\right). \end{aligned} \tag{11}$$

The FT of the three superposed JTH's will contain two correlation terms, one of which is

$$\begin{aligned}c_{apr} &= f(x, y - b) \star h_1(x, y - b) \\ &\quad + f(x, y - b)\exp\left[-i\left(\frac{2\pi}{3b}\right)(y - b)\right] \star h_2(x, y - b) \\ &\quad \times \exp\left[-i\left(\frac{2\pi}{3b}\right)(y - b)\right]\exp\left(i\,\frac{2\pi}{3}\right) \\ &\quad + f(x, y - b)\exp\left[-i\left(\frac{4\pi}{3b}\right)(y - b)\right] \star h_3(x, y - b) \\ &\quad \times \exp\left[-i\left(\frac{4\pi}{3b}\right)(y - b)\right]\exp\left(i\,\frac{4\pi}{3}\right). \end{aligned} \tag{12}$$

If $3b \gg 4\pi a$, where $2a$ is the maximum width of the input and filter, the linear phase factors can be neglected, leading to $f \star h$ as expected. In other words, the error can be neglected if the $|F||H_k|$ function variations are small compared to the spatial frequency of the fringes. In this way we take advantage of the optical FT to obtain the spectra, whereas the needed digital operations are simple and fast.

3. Laboratory and Simulation Experiments

A. Coherent Superposition

To demonstrate the feasibility of the procedure described in Subsection 2.A, a particular case of complex-valued function, a bipolar function was implemented. It consists of two slightly shifted delta functions with a π phase difference. It can be shown that correlating a two-dimensional function with such a reference results in a one-dimensional edge enhancement (see also Section 4). We demonstrate the implementation of the real bipolar-valued reference function, in this example, by decomposing the reference into two different positive-valued delta functions. Each of them is placed in a different channel of the interferometer shown in Fig. 2(a), and the superposition is performed coherently. In principle, the two delta functions could be implemented by using pinholes but, for the sake of light efficiency, small lenses were used to transform part of the beams in each interferometer arm into an approximate point source (delta function) at its focal plane. Optically this focal plane must coincide with the input plane. Only half of the input space is available in a JTC, so the lenses must have less than half of the dimension of the optical aperture. The proper phase difference is adjusted by the piezoelectrically mounted mirror, and the relative displacement of the point sources is chosen to obtain the desired resolution on an edge-enhanced image. Once the adjustment of the particular reference function is completed, the input function may be inserted and varied in real time if SLM's are employed.

Figure 3(a) shows the reconstruction of a conventional JTH for a rectangle as the input object by one

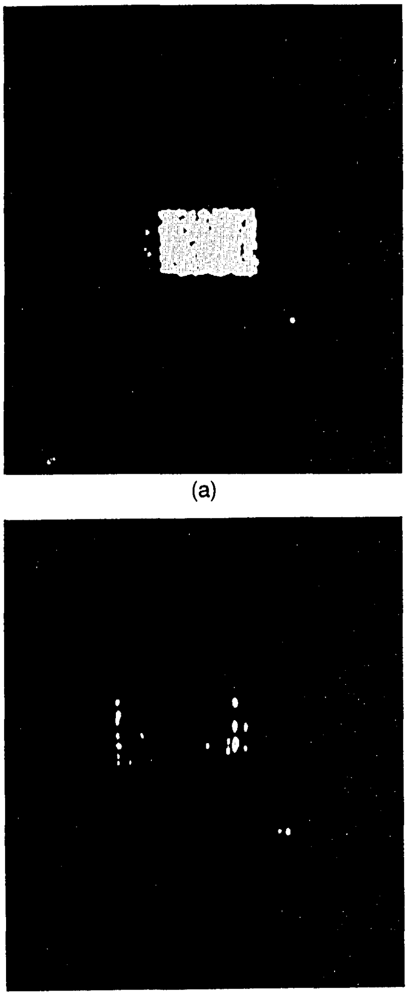

Fig. 3. Reconstructed images for a univalued rectangle: (a) conventional joint correlation with a delta function, (b) joint correlation with a bipolar filter for edge enhancement.

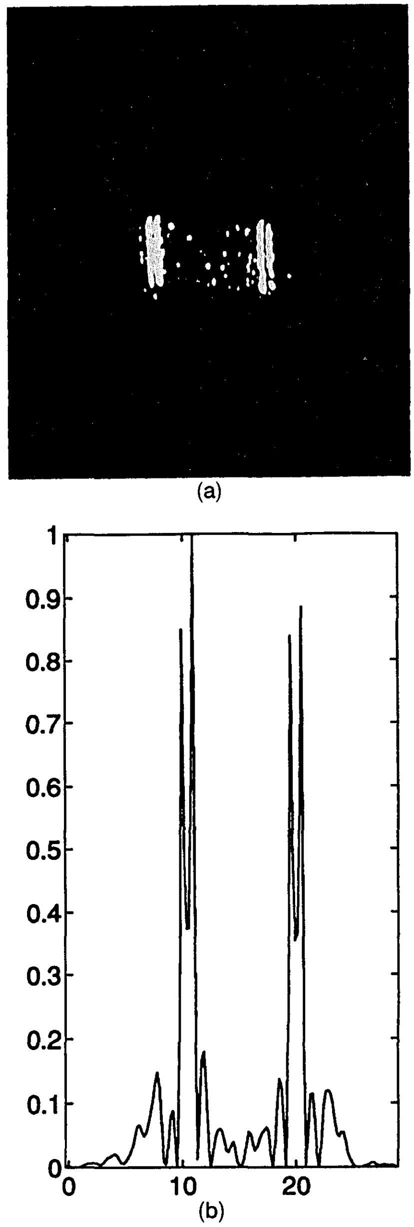

Fig. 4. Edge enhancement with nonlinearities in the JTH recording: (a) experimental result, (b) simulation with the same degree of saturation.

of the delta functions. The joint transform spectrum with the two point sources present is the coherent superposition of two interference patterns. A moiré pattern is generated, which causes selective cancellation of the information not associated with the edges. The edge enhancement of the object is thus obtained after reconstruction as shown in Fig. 3(b).

If the recording of the JTH is not linear, some interesting effects may occur. For example, overexposure, which results in saturation, leads to the reconstructed image shown in Fig. 4(a). The sharp bright line that marks the edge is replaced by a sharp dark line between two bright lines. This nonlinear effect was modeled and the simulated result is shown in Fig. 4(b).

B. Incoherent Superposition

The experiments described in Subsection 3.A were repeated with the incoherent method described in Subsection 2.B with similar results. The incoherent superposition in the Fourier plane is also demonstrated by the correlation between the letter E and its second-order circular harmonic component (CHC).[8]

Figures 5(a)–5(c) show the input consisting of the letter E in two rotated positions and the letter T, together with three different components h_k of the complex-valued CHC. Figures 5(d)–(f) display their respective JTH's, and Fig. 5(g) shows their superposition after translation in accordance with the approximate method described in Subsection 2.D. The simulated correlation output is shown in Fig. 5(h). As expected the letter E produces a correlation peak independent of the angular position, whereas the letter T produces a much lower and dispersed correla-

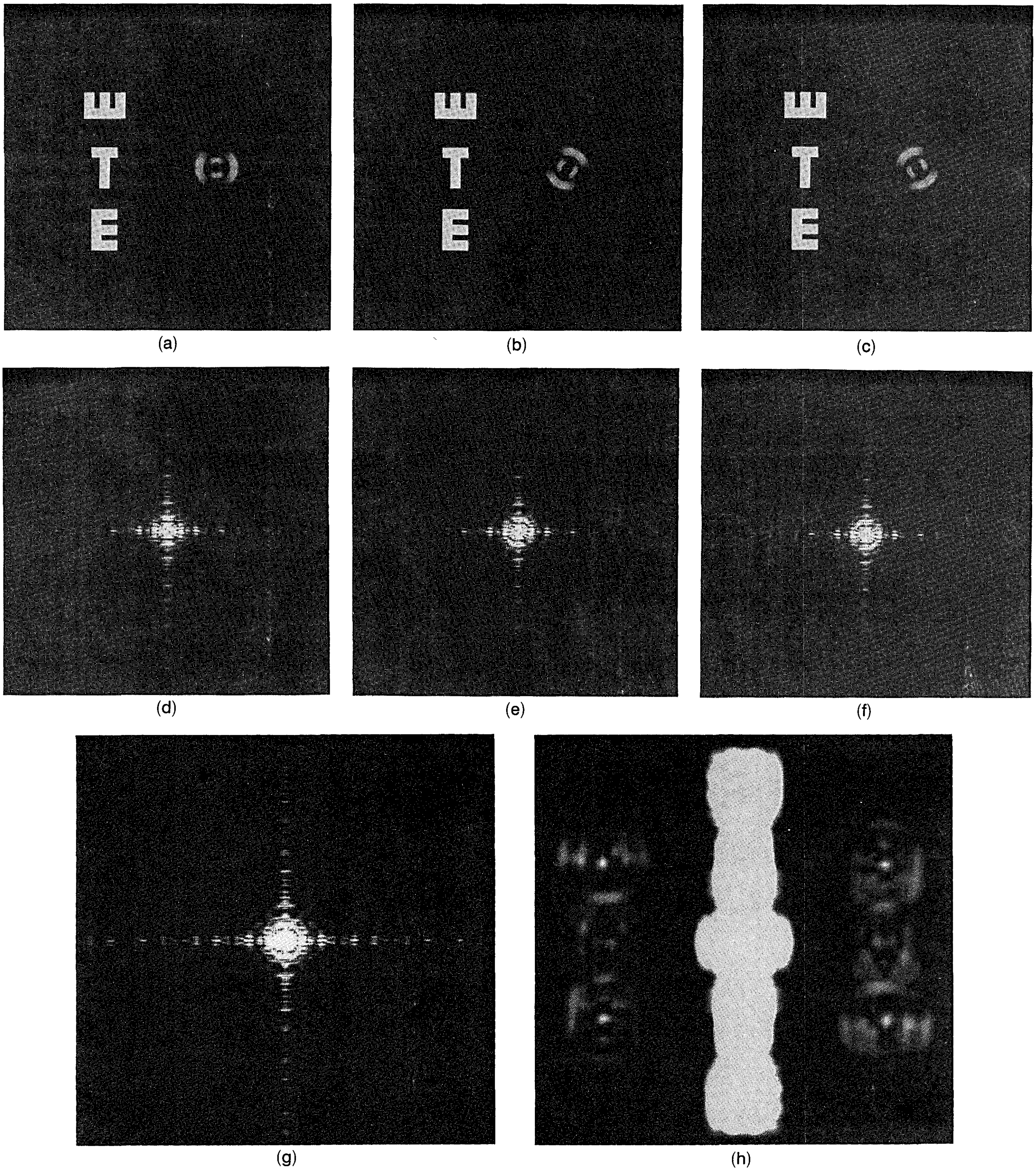

Fig. 5. Superposition at the Fourier plane correlation of an input pattern with a CHC of the letter E: (a)–(c) three components of the filter by the input, (d)–(f) three JTH's, (g) the JTH obtained after superposition (approximate solution), (h) the correlation output after Fourier transformation.

tion. This result can be compared to the exact solution shown in Fig. 6(d) to note the similarity in spite of the fact that the target and reference were relatively close.

Incoherent superposition at the output plane was performed with the same inputs as in Figs. 5(a)–(c). The spectra obtained [Figs. 5(d)–(f)] are Fourier transformed, and the correlations $c_k^2 = |f \star h_k|^2$ are

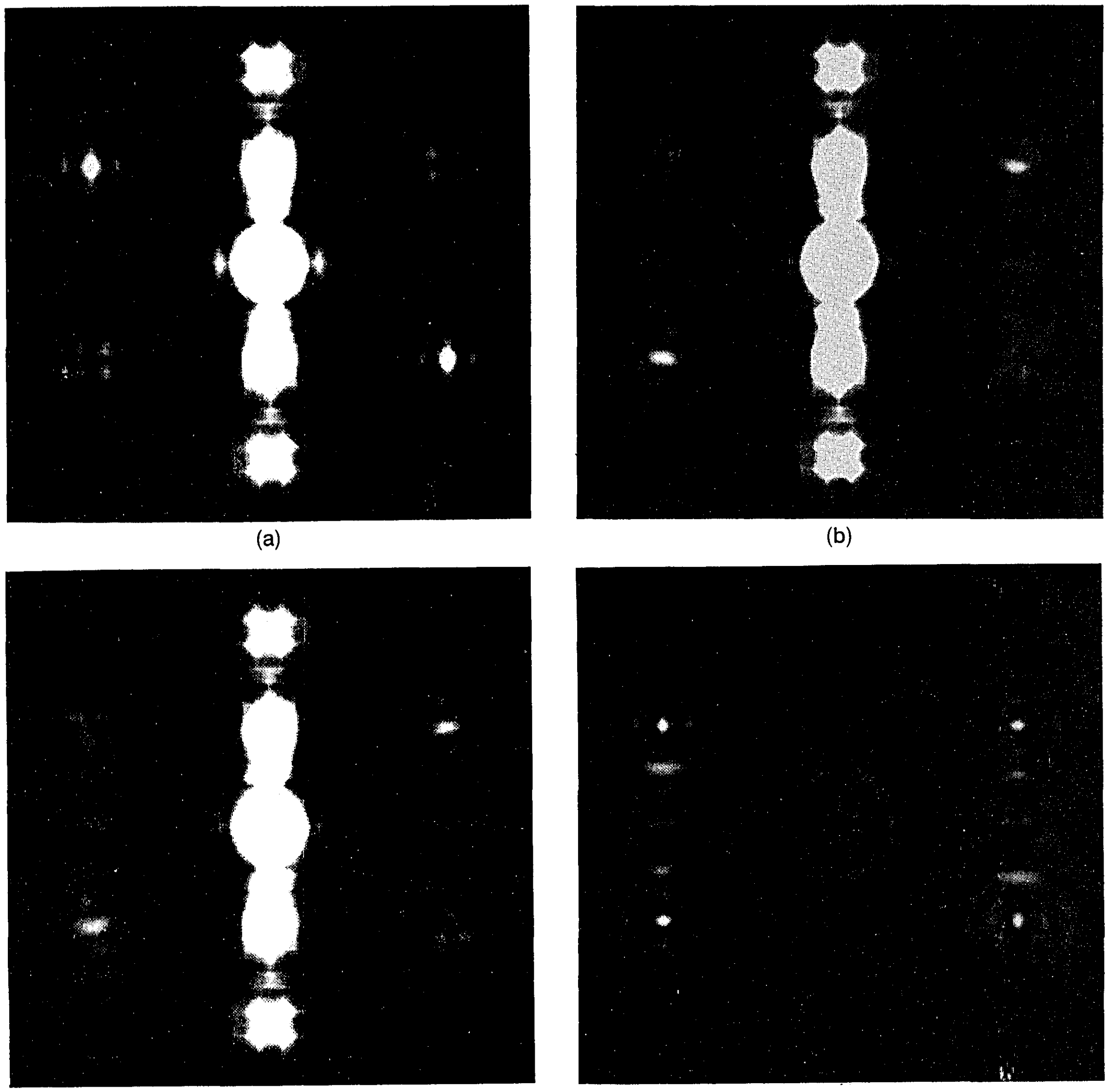

(a) (b) (c) (d)

Fig. 6. Incoherent superposition at the correlation plane. Correlation of an input pattern with a CHC of the letter E: (a)–(c) partial correlations of the three inputs from Figs. 5(a)–(c), (d) the final exact result after superposition.

shown in Figs. 6(a)–(c). The final result $|c|^2$ obtained after the superposition is performed according to Eq. (9) is displayed in Fig. 6(d). The zero order almost disappears because of the subtractions in Eq. (9).

4. Discussion and Conclusion

The three approaches investigated have their relative advantages and disadvantages. The superposition at the Fourier plane needs only two arms in the interferometer, which reduces alignment and stability problems. However, the procedure requires well-balanced multiple exposures and digital postprocessing that is not so suitable for real-time applications. The approximate implementation discussed in Subsection 2.D is adequate for most applications, but at the expense of partial loss of shift invariance in one direction.

Coherent superposition at the input plane, on the other hand, is implemented in real time, but the optical system is more complicated and subject to alignment problems and interferometric noise.

Incoherent superposition at the correlation plane is probably the most robust technique, since no precise phases or translations are needed. The digital processing is simple but still more complex than in the other techniques.

Preliminary results of a bipolar filter for edge enhancement and a CHC reference function for JTC applications are promising. The principle can be extended beyond the JTC applications. For example, the third method described in Subsection 2.D in its coherent and incoherent form can be adapted to the $4f$ correlator with the same bandwidth advantage.

In conclusion, new methods for continuous complex function generation for a JTC have been proposed. The techniques presented may be considered as a class of holographic representations with no reference beams. They have the potential to develop or emulate complex continuous wave fronts in an on-axis configuration at the input plane. As opposed to classical holography for which higher orders are obtained, only a zero order is attained in this case, reducing the space–bandwidth requirements of the recording media. The filter decomposition into three functions reduces the noise at the output, as compared to the decomposition into two functions, and saves memory space and time as compared to the decomposition into four functions.

Since the component functions are real, SLM's can be used and thus computer control of the process can be implemented.

This work was performed within the Technion Advanced Opto-Electronics Center established by the American Technion Society, New York. J. Rosen was a National Research Council Research Associate at Rome Laboratory while this work was performed.

References

1. C. S. Weaver and J. W. Goodman, "A technique for optically convolving two functions," Appl. Opt. **5,** 1248–1249 (1966).
2. D. Mendlovic, E. Marom, and N. Konforti, "Complex reference-invariant joint-transform correlator," Opt. Lett. **15,** 1224–1226 (1990).
3. U. Mahlab, J. Rosen, and J. Shamir, "Iterative generation of complex reference functions in a joint-transform correlator," Opt. Lett. **16,** 330–332 (1991).
4. J. Rosen, U. Mahlab, and J. Shamir, "Complex reference discriminant functions implemented iteratively on a joint transform correlator," Appl. Opt. **30,** 5111–5115 (1991).
5. J. W. Goodman and L. M. Woody, "Performing complex-valued linear operations on complex-valued data using incoherent light," Appl. Opt. **16,** 2611–2612 (1977).
6. P. Chavel and J.-P. Hugonin, "High quality computer holograms: the problem of phase representation," J. Opt. Soc. Am. **66,** 989–996 (1976).
7. F. T. S. Yu, X. Li, E. C. Tam, S. Jutamulia, and D. A. Gregory, "Rotation invariant pattern recognition with a programmable joint transform correlator," Appl. Opt. **28,** 4725–4727 (1989).
8. Y.-N. Hsu and H. H. Arsenault, "Optical pattern recognition using circular harmonic expansion," Appl. Opt. **21,** 4016–4019 (1982).